J Neurophysiol 115: 2446–2455, 2016.
First published February 24, 2016; doi:10.1152/jn.00566.2015.

$mGlu_1$ receptor mediates homeostatic control of intrinsic excitability through I_h in cerebellar Purkinje cells

Hyun Geun Shim,[1,2] Sung-Soo Jang,[1,3] Dong Cheol Jang,[1,4] Yunju Jin,[5] Wonseok Chang,[6] Joo Min Park,[5]* and Sang Jeong Kim[1,2,3]*

[1]*Department of Physiology, Seoul National University College of Medicine, Seoul, Republic of Korea;* [2]*Department of Biomedical Science, Seoul National University College of Medicine, Seoul, Republic of Korea;* [3]*Neuroscience Research Institute, Seoul National University College of Medicine, Seoul, Republic of Korea;* [4]*Department of Brain and Cognitive Sciences, College of Science, Seoul National University, Kwanak-gu, Seoul, Republic of Korea;* [5]*Center for Cognition and Sociality, Institute for Basic Science (IBS), Daejeon, Republic of Korea; and* [6]*Department of Anesthesiology, Duke University Medical Center, Durham, North Carolina*

Submitted 9 June 2015; accepted in final form 21 February 2016

Shim HG, Jang SS, Jang DC, Jin Y, Chang W, Park JM, Kim SJ. $mGlu_1$ receptor mediates homeostatic control of intrinsic excitability through I_h in cerebellar Purkinje cells. *J Neurophysiol* 115: 2446–2455, 2016. First published February 24, 2016; doi:10.1152/jn.00566.2015.— Homeostatic intrinsic plasticity is a cellular mechanism for maintaining a stable neuronal activity level in response to developmental or activity-dependent changes. Type 1 metabotropic glutamate receptor ($mGlu_1$ receptor) has been widely known to monitor neuronal activity, which plays a role as a modulator of intrinsic and synaptic plasticity of neurons. Whether $mGlu_1$ receptor contributes to the compensatory adjustment of Purkinje cells (PCs), the sole output of the cerebellar cortex, in response to chronic changes in excitability remains unclear. Here, we demonstrate that the $mGlu_1$ receptor is involved in homeostatic intrinsic plasticity through the upregulation of the hyperpolarization-activated current (I_h) in cerebellar PCs. This plasticity was prevented by inhibiting the $mGlu_1$ receptor with Bay 36–7620, an $mGlu_1$ receptor inverse agonist, but not with CPCCOEt, a neutral antagonist. Chronic inactivation with tetrodotoxin (TTX) increased the components of I_h in the PCs, and ZD 7288, a hyperpolarization-activated cyclic nucleotide-gated channel selective inhibitor, fully restored reduction of firing rates in the deprived neurons. The homeostatic elevation of I_h was also prevented by BAY 36–7620, but not CPCCOEt. Furthermore, KT 5720, a blocker of protein kinase A (PKA), prevented the effect of TTX reducing the evoked firing rates, indicating the reduction in excitability of PCs due to PKA activation. Our study shows that both the $mGlu_1$ receptor and the PKA pathway are involved in the homeostatic intrinsic plasticity of PCs after chronic blockade of the network activity, which provides a novel understanding on how cerebellar PCs can preserve the homeostatic state under activity-deprived conditions.

homeostatic plasticity; intrinsic excitability; $mGlu_1$ receptor; I_h

HOMEOSTATIC INTRINSIC PLASTICITY maintains the stability of neuronal network activity against environmental or pathological destabilization, which includes the modulation of postsynaptic neurotransmitter receptors and the differential expression of ion channel genes (Desai et al. 1999; Lee et al. 2015; Naude et al. 2013). It therefore serves as a basis for the neural network to achieve an optimal activity range. Intrinsic cellular excitability, in particular, determines the total output of a neuron by integrating synaptic inputs and consecutively translating them into the firing of an action potential (AP). Thus, homeostatic intrinsic excitability plays a pivotal role in maintaining the network balance and maximizing information storage by tuning the average firing rate through the modulation of multiple neurotransmitter receptors and voltage-dependent channels (Stemmler and Koch 1999). Homeostatic intrinsic plasticity is a fascinating model on the plastic changes in neural circuits in both physiological and pathological conditions (Beraneck and Idoux 2012; Lambo and Turrigiano 2013; O'Leary et al. 2014). However, much of the detailed cellular and molecular basis for these regulatory mechanisms is largely unknown.

Metabotropic glutamate (mGlu) receptors monitor neuronal activity and can trigger either Hebbian or homeostatic synaptic plasticity using similar intracellular signaling cascades including calcium influx as well as induction of the immediate early gene Homer1a (Hu et al. 2010), Arc (Shepherd et al. 2006), and eukaryotic elongation factor 2 (Sutton et al. 2007). In addition, altered synaptic activity can also result in mGlu1 receptor-dependent changes in intrinsic excitability (Brager and Johnston 2007). A recent study (Lee et al. 2015) identified mGlu receptors among 873 novel chronic activity-regulated transcripts that had not previously been implicated in homeostatic intrinsic plasticity. Given the similarity in signaling between Hebbian and homeostatic synaptic plasticity, homeostatic regulation of intrinsic excitability could share a signal cascade with intrinsic plasticity following the Hebbian rule. Thus, we investigated whether $mGlu_1$ receptors contribute to homeostatic intrinsic plasticity. We hypothesized that the type 1 metabotropic glutamate receptor ($mGlu_1$ receptor) activity contributes to homeostatic intrinsic plasticity. To test this, we prepared organotypic slice cultures of rat cerebellum obtained by the membrane interface method and measured neuronal activities of Purkinje cells (PCs) by electrophysiological recordings. We found that the intrinsic excitability of cerebellar PCs was reduced by chronic activity deprivation. An $mGlu_1$ receptor inverse agonist but not a neutral antagonist prevented these homeostatic changes, suggesting that the constitutive activation of the $mGlu_1$ receptor results in decreases in intrinsic excitability. In addition, prolonged activity deprivation robustly increased the hyperpolarization-activated current (I_h) components, and the reduced excitability was rescued by an I_h antagonist, suggesting that the homeostatic intrinsic plasticity

* J. M. Park and S. J. Kim are cosenior authors of this work.
Address for reprint requests and other correspondence: S. J. Kim, Dept. of Physiology, Seoul Natl. Univ. College of Medicine, 28 Yeongeon-dong, Jongno-gu, Seoul, 110-799, Republic of Korea (e-mail: sangjkim@snu.ac.kr).

was dependent on I_h. The antagonism of the $mGlu_1$ receptor also blocked the homeostatic upregulation of I_h and consequently attenuated the intrinsic excitability. Our observations indicate that homeostatic intrinsic excitability in cerebellar PCs is mediated by the agonist-independent activity of the $mGlu_1$ receptor through regulation of I_h.

MATERIALS AND METHODS

Slice preparation and organotypic slice culture. Experiments were performed according to methods approved by the Institutional Animal Care and Use Committee of Seoul National University College of Medicine and were in accordance with the ethical standards of the institutional research committee. After brain dissection, 250 μm cerebellar sagittal slices were made with a vibrating tissue slicer (Microm HM 650V) in ice-cold standard artificial cerebrospinal fluid (aCSF) solution: (in mM) 124 NaCl, 2.5 KCl, 1 NaH_2PO_4, 1.3 $MgCl_2$, 2.5 $CaCl_2$, 26.2 $NaHCO_3$, and 20 D-glucose, bubbled with 95% O_2/5% CO_2, pH 7.4. Sagittal planes of cerebellar slices were transferred onto membrane of culture insert (pore size 0.4 μm) in six-well plastic plates. Culture medium (1 ml), composed of 50% basal medium with Earle's salts, 25% HBSS, 25% heat-inactivated horse serum, 1% L-glutaMaxTM-1 and 5 mg/ml glucose, was added into each well below the culture inserts. Cultured slices were incubated at 35°C in an atmosphere of humidified 5% CO_2, and half of medium was replaced every 2–3 days.

Western blot analysis. For Western blot, cultured slices were homogenized with homogenizing buffer (1% Triton X100, 0.1% SDS, 50 mM Tris·HCl, 0.3 M sucrose, 5 mM EDTA with protease inhibitor cocktail and pH 7.5) on ice. Lysates were boiled for 2 min at 60°C and loaded by 4–12% gradient SDS-PAGE gel. Separated proteins were transferred to PVDF membrane. The membrane blocked with 5% skim milk in TBS-T (24.7 mM Tris, 137 mM NaCl, 2.7 mM KCl, and 1% Tween 20, pH 7.4) for 1 h and incubated with anti-$mGlu_1$ receptor-α (anti-mouse, 1:2,000, BD Bioscience), anti-β-actin (anti-mouse, 1:3,000, Sigma) for additional 1 h. After being washed with TBS-T, the membrane was incubated overnight at 4°C with horseradish peroxidase-conjugated appropriate goat IgG (1:2,000, Stressgen). The immunoblots were developed with enhanced chemiluminescence (ECL) solution (Invitrogen). For quantifying the band, Quantity One (Bio-Rad) was used.

Electrophysiology. Whole cell patch-clamp configurations were made from 10–12 days in vitro slices. Slices were put onto a submerged recording chamber on the stage of Olympus microscope (BX50WI) and perfused with aCSF at 32°C and kept in place with a nylon-strung platinum anchor. All recordings were performed using multiclamp 700B patch-clamp amplifier (Axon Instruments) with a sampling frequency of 20 kHz, and signals were filtered at 2 kHz. For current clamp experiments, standard aCSF was used as extracellular solution described above; for voltage clamp experiments to isolate I_h, slices were incubated with extracellular solution composed of (in mM) 115 NaCl, 1.2 NaH_2PO_4, 5 KCl, 2 $CaCl_2$, 1 $MgCl_2$, 25 $NaHCO_3$, 20 glucose, 1 $BaCl_2$, 5 tetraethyl ammonium (TEA), 1 4-aminopyrimidine (4-AP), 1 $NiCl_2$, 0.1 $CdCl_2$, 0.01 μM 2,3-dihydroxy-6-nitro-7-sulfamoyl-benzo[f]quinoxaline-2,3-dione (NBQX), 0.1 picrotoxin, and 0.0005 tetrodotoxin (TTX), bubbled with 90% O_2, 5% CO_2, pH 7.4 (Nolan et al. 2003). Both excitatory and inhibitory synaptic inputs were all blocked by 10 μM NBQX and 100 μM picrotoxin, respectively. Patch pipettes (3–4 MΩ) were borosilicate glass and filled with internal solution containing (in mM), 9 KCl, 10 KOH, 120 K-gluconate, 3.48 $MgCl_2$, 10 HEPES, 4 NaCl, 4 Na_2ATP, 0.4 Na_3GTP, and 17.5 sucrose, pH adjusted to 7.25. Electrophysiological recordings were started 5 min after obtaining the whole cell configuration to let the internal solution diffuse enough into the cytosol.

Data acquisition and analysis. All data were acquired by Clampex software (Molecular Devices) and analyzed by IgorPro 8.1 (Wavemetrics). Otherwise we note, a cell was clamped at −70 mV with current injection and neurons with the injection current below −500 pA were discarded from this analysis. To evaluate the PC excitability, a series of current steps of 1 s duration ranging from +100 to +500 pA in 100 pA increments with a step interval of 4.5 s was applied to the cell from the membrane potential of −70 mV. Input resistance (R_{in}) was measured by injecting brief current (−200 pA or +100 pA; 100 ms) and was determined from the negative peak voltage deflection during current injection. Voltage threshold ($V_{threshold}$) of AP was defined as the voltage where the dV/dt first exceeds 30–60 mV/ms. Membrane capacitance (C_m) was calculated by $C_m = \tau/R$, at which the time constant (τ) and series resistance (R_S) were calculated fitting a single exponentials to the voltage responses of the test pulse (−5 mV). Resting membrane potential (V_m) was measured when injected current was absent in current clamp mode with 1 μM TTX to prevent spontaneous AP firing. The AP waveform, including AP amplitude, half-width, 10–90% rise time, and first spike latency, was analyzed from the first evoked AP of the firing train when +400 pA of the depolarizing current was injected. AP amplitude was determined as difference between peak amplitude and the voltage threshold of the AP. Half-width and 10–90% rise time were the time duration at the half-maximal voltage, elevation time from 10 to 90% of the maximal AP voltage, respectively. The first spike latency was defined as the delay from beginning point of depolarizing current injection to the voltage threshold where the upstroke phase of the first spike was initiated. Fast afterhyperpolarization (fAHP) and medium afterhyperpolarization (mAHP) were measured by calculating the difference between voltage threshold and hyperpolarized negative peak voltage after the first AP or depolarizing square current injection, respectively.

The amount of voltage sag determined as difference between the maximum and steady-state voltage during the hyperpolarizing current injection from −100 pA to −600 pA with increments of −100 pA for 1 s with a step interval of 5 s. This sag amplitude was converted to sag percent, representing percentage change between two states $[(V_{Max} - V_{Steady\ state})/V_{Max}] \times 100$. For I_h current isolation in voltage clamp, membrane potential was held at −45 mV and step voltage was applied from −50 mV to −120 mV with increments of −5 mV of 2.5 s.

Data are presented as means ± SE, and statistical evaluations were performed by two-sample *t*-test, two-way repeated-measures ANOVA with post hoc Tukey's test and Mann-Whitney *U*-test by Origin 8.5 and SigmaPlot 12.0 software, and the normal distribution was verified.

RESULTS

Rat organotypic cerebellar cultures were used rather than primary culture neurons to better preserve in vivo circuits. To investigate homeostatic intrinsic plasticity in cerebellar PCs, network activity of the cerebellar cortex was chronically deprived by applying TTX (1 μM) for 2 days (Fig. 1*A*). Evoked AP firing rates of control and TTX-treated (deprived) PCs in the presence of excitatory and inhibitory synaptic blockers were compared by injecting brief current steps from the membrane potential of about −70 mV (1 s, from +100 pA to +500 pA with an increment of 100 pA, step interval 4.5 s, see MATERIALS AND METHODS). Activity deprivation reduced the intrinsic excitability of the PCs over most ranges of the current injection [Fig. 1*B*; firing frequency (Hz): control = 31.2 ± 1.7 at 400 pA injection, $n = 24$; deprived = 20.4 ± 1.9, $n = 20$; control vs. deprived: $P < 0.001$, two-way repeated-measured ANOVA]. The active properties of the neurons were analyzed from the first spike of the evoked spike train when +400 pA current was injected (Fig. 1*C*, Table 1). Activity deprivation increased the current threshold ($I_{threshold}$) for evoking spikes, whereas $V_{threshold}$ did not change [$I_{threshold}$ (pA): control = 200.6 ± 10.7; deprived = 235 ± 8.2; control vs. deprived: $P < 0.05$; $V_{threshold}$ (mV): control = −40.2 ± 1.0; deprived =

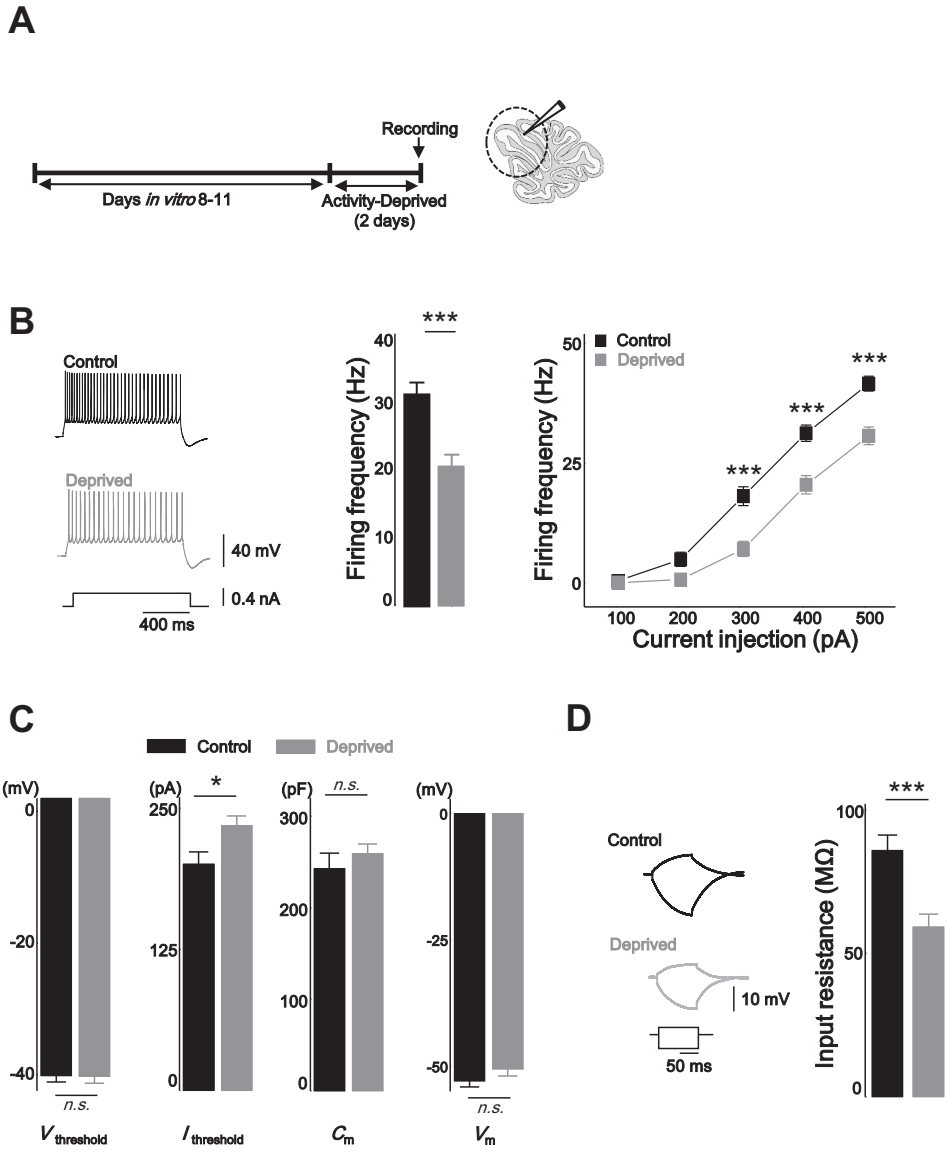

Fig. 1. Chronic activity deprivation decreased intrinsic excitability of cerebellar Purkinje cells (PCs). *A*: experimental scheme. Network activity totally deprived by treatment of 1 μM tetrodotoxin (TTX) for 2 days in organotypic cerebellar slice culture. Electrophysiological recording was performed at anterior lobule (*lobule III–V*). *B*: representative traces (*left*), bar graphs at +400 pA injection (*middle*), and plots (*right*) showing that chronic activity-deprivation decreased intrinsic excitability of PCs. *C*: bar graph showing that chronic activity deprivation increased current threshold ($I_{threshold}$), but voltage threshold ($V_{threshold}$), membrane capacitance (C_m), and membrane potential (V_m) were not changed. *D*: representative traces (*left*) and summarizing graph (*right*) showing the input resistance (R_{in}) was decreased after chronic activity deprivation. Black, control; gray, deprived. Asterisks in *B* marked by post hoc Tukey's test, pairwise comparison followed by 2-way repeated-measures ANOVA; $*P < 0.05$, $***P < 0.001$; n.s., no significance.

−40.3 ± 1.0; control vs. deprived: $P = 0.95$]. The passive membrane properties C_m and V_m were not altered by activity deprivation [C_m (pF): control = 242.6 ± 17.2; deprived = 259.1 ± 10.4; control vs. deprived: $P = 0.4$, V_m (mV): control = −52.9 ± 1.2; deprived = −50.6 ± 1.4; control vs. deprived: $P = 0.2$]. To measure R_{in}, voltage response was monitored when brief hyperpolarizing and subthreshold depolarizing current (−200 pA and +100 pA) were injected in the current clamp mode (Fig. 1*D*). R_{in} was significantly reduced in deprived neurons, and subsequently, voltage deflection was less in response to a brief input current (control = 85.8 ± 5.4 MΩ; deprived = 59.2 ± 4.5 MΩ; control vs. deprived: $P < 0.001$). The AP waveform, which included the AP amplitude (control = 55.3 ± 1.0 mV; deprived = 57.8 ± 1.0 mV), the half-width (control = 0.39 ± 0.01 ms; deprived = 0.39 ± 0.01 ms) and AP rise time (control = 0.25 ± 0.01 ms; deprived =

Table 1. *Parameters of AP properties and waveform*

	$V_{threshold}$, mV	$I_{threshold}$, pA	AP Amplitude, mV	Half-width, ms	Rise Time, ms	First Spike Latency, ms	fAHP, mV	mAHP, mV	R_{in}, MΩ	V_m, mV	C_m, pF
Control	−40.2 ± 1.0	200.6 ± 10.7	55.3 ± 1.0	0.4 ± 0.01	0.25 ± 0.05	24.6 ± 1.6	10.3 ± 0.8	9.8 ± 0.7	85.8 ± 5.4	−52.9 ± 1.2	241.6 ± 17.2
Deprived	−40.3 ± 1.0	235.0 ± 8.2*	57.8 ± 1.0	0.4 ± 0.01	0.22 ± 0.01	28.8 ± 2.1	9.3 ± 1.0	12.7 ± 0.9*	59.2 ± 4.5***	−50.6 ± 1.4	259.1 ± 10.4

Among active membrane properties, current threshold ($I_{threshold}$) was increased under deprived condition, whereas voltage threshold ($V_{threshold}$) was not changed (see also Fig. 1). Action potential (AP) waveform, including AP amplitude, half-width, 10–90% rise time, and first spike latency, was monitored. The parameters were not affected by activity deprivation. Medium afterhyperpolarization (mAHP) was increased in deprived neurons, whereas fast afterhyperpolarization (fAHP) was not altered. Among the passive membrane properties [membrane capacitance (C_m), membrane potential (V_m), and input resistance (R_{in})], only R_{in} was changed by activity deprivation. For comparison of the active and passive membrane properties, changes described here are from those shown in Fig. 1, *C* and *D*. $*P < 0.05$, $***P < 0.001$.

0.22 ± 0.01), first spike latency (control = 24.6 ± 1.7 ms; deprived = 28.8 ± 2.1 ms), and fAHP (control = 10.3 ± 0.8; deprived = 9.3 ± 1.0), was not altered in the activity-deprived condition (Table 1). mAHP was increased in the deprived neuron (Table 1; control = 9.8 ± 0.7; deprived = 12.7 ± 0.9; control vs. deprived: $P < 0.05$, statistical evaluation of all active and passive properties were done by two-sample *t*-test).

The mGlu receptor can induce plasticity of the intrinsic excitability by initiating a signal cascade resulting in the regulation of ion channels such as I_h, Ca^{2+} channel, and K^+ channels (Brager and Johnston 2007; Kammermeier et al. 2000). Interestingly, agonist-independent (constitutive) activation of mGlu receptor is required for homeostatic synaptic plasticity, suggesting interplay between Hebbian and homeostatic synaptic plasticity (Hu et al. 2010). It has been unclear whether homeostatic intrinsic plasticity also requires agonist-independent activation of the $mGlu_1$ receptor from a homeostatic perspective. To test the hypothesis that the constitutive activity of the $mGlu_1$ receptor acts as the mechanism for the TTX-induced attenuated firing rates, the protein level of the $mGlu_1$ receptor was assessed by Western blot. The expression level of mGlu receptors may change if these receptors contribute to homeostatic intrinsic plasticity because the facilitated agonist-independent activity of G protein-coupled receptors (GPCRs) corresponds with increased protein level (Smit et al. 1996). In addition, it has been observed that $mGlu_1$ receptor expression is regulated in response to changes in network activity (Ehlers 2003). Consistent with this hypothesis, $mGlu_1$ receptor expression was increased by activity deprivation (Fig. 2*A*; control vs. deprived: $P < 0.05$, Mann-Whitey *U*-test). To further examine our hypothesis, $mGlu_1$ receptor inverse agonist, (3aS,6aS)-Hexahydro-5-methylene-6a-(2-naphthalenylmethyl)-1H-cyclopenta[c]furan-1-one (BAY 36–7620) (10 μM), or neutral antagonist, 7-(hydroxyimino)cyclopropa[b]chromen-1a-carboxylate ethyl ester (CPCCOEt) (100 μM) was applied for 2 days to control and TTX-treated slices (Fig. 2*B*). Inverse agonist BAY 36–7620 (BAY) binds within the transmembrane domain of $mGlu_1$ receptor and stabilizes the receptor in the inactive form (Nakashima et al. 2013). On the other hand, the other agent, CPCCOEt (CP), is classified as a neutral, noncompetitive antagonist that inhibits agonist binding in the NH_2 terminus and suppression of agonist-induced signaling (Ango et al. 2001; Litschig et al. 1999). Blockade of the $mGlu_1$ receptor with the inverse agonist prevented homeostatic intrinsic plasticity induced by chronic TTX treatment [Fig. 2*C*; control + BAY: firing frequency (Hz) = 34.3 ± 2.9 at 400 pA injection, $n = 11$; deprived + BAY: firing frequency (Hz) = 33.9 ± 1.8, $n = 13$; control vs. control + BAY: $P = 0.31$; deprived vs. deprived + BAY: $P < 0.05$, two-way repeated-measured ANOVA], whereas the homeostatic downregulation of firing rates was not prevented by the neutral antagonist (Fig. 2*D*; control + CP: firing frequency = 31.4 ± 2.2 at 400 pA injection, $n = 11$; deprived + CP: firing frequency = 23.0 ± 3.1, $n = 10$; control vs. control + CP: $P = 0.69$; deprived vs. deprived + CP: $P = 0.58$, two-way repeated-measured ANOVA). The R_{in} of the control and deprived slices was measured after treatment with BAY or CP for 2 days. Consistent with the results of the firing rates in Fig. 2, *C* and *D*, the antagonisms of the $mGlu_1$ receptor by the inverse agonist prevented homeostatic downregulation of R_{in} (BAY: control + BAY = 86.1 ± 6.1 MΩ; deprived + BAY = 83.8 ± 5.7 MΩ; $P > 0.05$; control + CP = 90.6 ± 5.8 MΩ; deprived + CP = 74.9 ± 2.8 MΩ; $P < 0.05$, two-sample *t*-test; Fig. 2*E*). Taken together, our observation suggests that the homeostatic intrinsic plasticity of PCs requires the agonist-independent action of the $mGlu_1$ receptor.

From the parameters of the AP waveform (Table 1), we found that the prolonged inhibition of the network activity robustly decreased the R_{in}, and consequently, excitability was downregulated (Figs. 1, *C* and *D*, and 2*E*). Among the various ion channels, we examined the hyperpolarization-activated cyclic nucleotide gated (HCN) channel because it has been widely postulated that I_h modulates the cellular excitability via contributing to R_{in} (Brager and Johnston 2007; Campanac et al. 2008; Rosenkranz and Johnston 2006). We speculated that activity deprivation caused the upregulation of I_h, resulting in reduced intrinsic excitability after chronic TTX treatment. Voltage sag and rebound depolarization were measured by hyperpolarizing step current injection (from −100 pA to −600 pA with an increment of −100 pA for 1 s with a step interval of 5 s) in the current clamp mode (Fig. 3, *A* and *C*). The voltage sag was normalized by the maximal negative voltage then recalculated as a percentage (Fig. 3*B*). In deprived neurons, all I_h components were elevated [voltage sag (mV): control = 6.7 ± 0.6 at −400 pA injection, $n = 12$; deprived = 10.2 ± 0.8 at −400 pA injection, $n = 14$; control vs. deprived: $P < 0.05$, two-way repeated-measured ANOVA; sag % (%): control = 24.0 ± 1.8; deprived = 40.3 ± 2.2 at −400 pA injection; $P < 0.001$, two-sample *t*-test; rebound depolarization: control = 4.0 ± 0.3; deprived = 7.3 ± 0.6 at −400 pA injection; $P < 0.001$, two-sample *t*-test]. We also observed the elevation of I_h in deprived neurons in the voltage clamp configuration (Fig. 3*D*; control I_h density = −1.0 ± 0.1 pA/pF at $V_m = -100$ mV, $n = 15$; deprived I_h density = −1.5 ± 0.1 pA/pF, $n = 14$; control vs. deprived: $P < 0.05$, two-way repeated-measures ANOVA). The tail current was normalized to the maximal amplitude, and then, the resulting data were fitted with a Boltzmann function (Fig. 3*E*). The half-maximal voltage ($V_{50\%}$) was not shifted (control = 84.9 ± 0.5 mV; deprived = −85.9 ± 0.8 mV), suggesting that voltage dependency was not affected by activity deprivation.

To test whether the downregulation of intrinsic excitability resulted from the elevation of I_h, the firing rates of the control and deprived neurons were compared before and after applying 4-ethylphenylamino-1,2-dimethyl-6-methylaminopyrimidinium chloride (ZD 7288), an HCN channel selective inhibitor (Fig. 4*A*). Indeed, the decrease in the excitability of the deprived neurons was fully restored by I_h inhibition [control: pre firing frequency (Hz) = 26.7 ± 4.3, ZD 7288 = 45.4 ± 3.5; deprived: before firing frequency (Hz) = 11.7 ± 2.5, after = 46.7 ± 2.1]. R_{in} was robustly increased in neurons treated with ZD 7288; the difference between the control and deprived neurons was indisputably abolished by ZD 7288 [Fig. 4*B*; control: pre-ZD 7288 R_{in} (MΩ) = 89.3 ± 6.7, post-ZD 7288 = 224.2 ± 23.5, $n = 6$; deprived: pre-ZD 7288 R_{in} = 60.6 ± 6.0, post-ZD 7288 = 178.2 ± 9.7, $n = 5$; pre-ZD 7288 $P < 0.05$, post-ZD 7288 $P = 0.12$, two-sample *t*-test]. Thus, we conclude that homeostatic intrinsic plasticity in cerebellar PCs requires I_h regulation.

We asked whether homeostatic upregulation of I_h was dependent on the agonist-independent activity of the $mGlu_1$

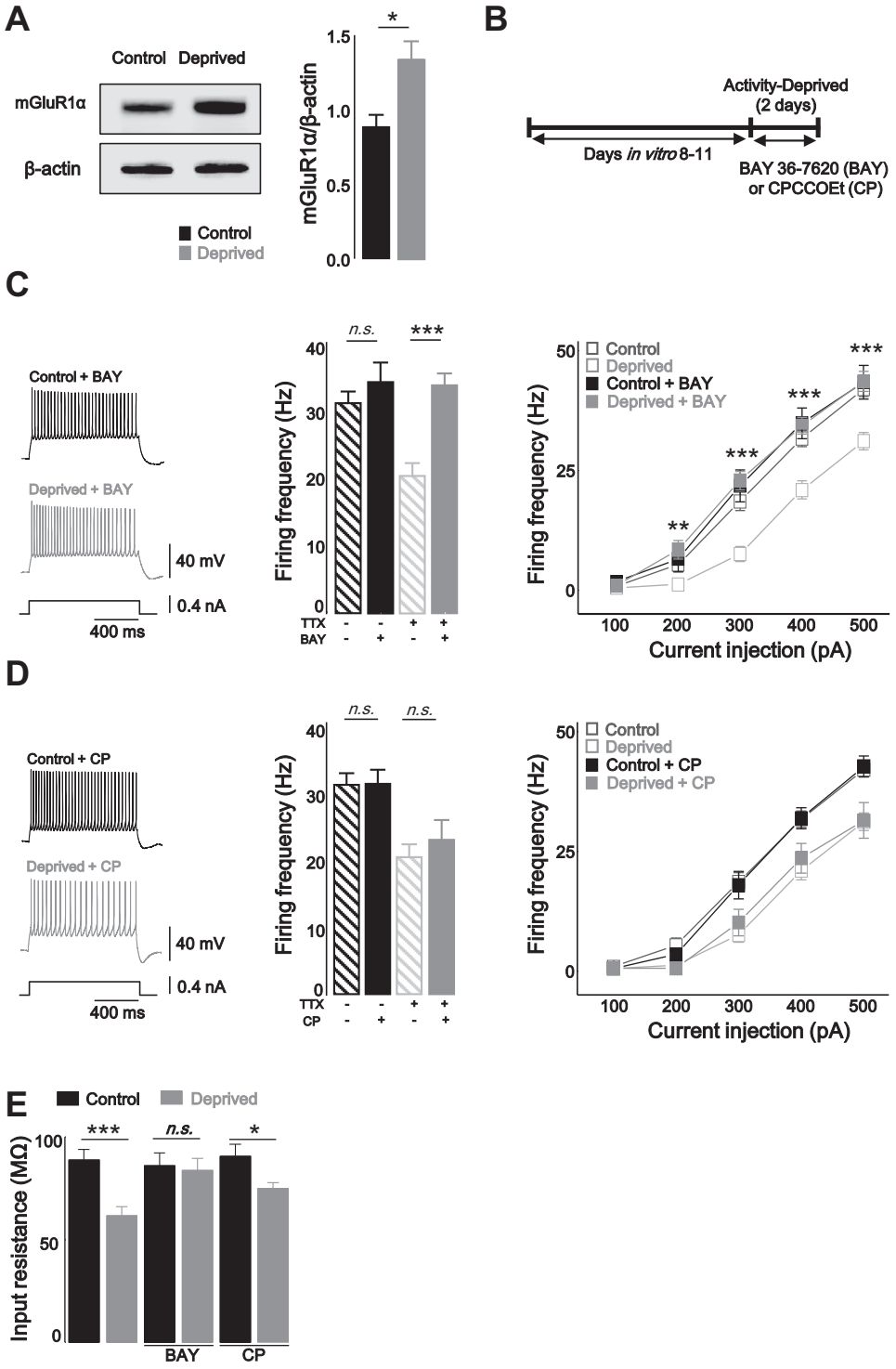

Fig. 2. Homeostatic intrinsic plasticity of cerebellar PCs was required to agonist-independent activity of type 1 metabotropic glutamate receptor (mGlu$_1$R). *A*: immunoblotting of mGlu$_1$ receptor-α (mGluR1α) from control and deprived neuron (*left*) and summarizing bar graphs (*right*) showing that chronic activity deprivation increased the protein level of mGlu$_1$Rα. *B*: experimental scheme. mGlu$_1$ receptor inhibitors, BAY 36–7620 (BAY) or CPCCOEt (CP), were treated for 2 days in presence or absence of TTX. *C*: representative traces (*left*), summarizing bar graphs (*middle*; at +400 pA injection), and plots (*right*) showing that inverse agonist of mGlu$_1$ receptor inhibited induction of homeostatic intrinsic plasticity. Closed black square, BAY only; closed gray square, deprived + BAY; open black square, control; open gray square, deprived. Control and deprived values are described in Fig. 1. *D*: representative traces (*left*) and summarizing bar graphs (*middle*; at +400 pA injection), and plots (*right*) showing that there were no effects of antagonizing mGlu$_1$ receptor by CP on homeostatic intrinsic plasticity. Closed black square, CP only; closed gray square, deprived + CP; open black square, control; open gray square, deprived. Control and deprived values are as described in Fig. 1. *E*: bar graph showing that reduced R_{in} was recovered by inverse agonist, BAY, and neutral antagonist, CP, was not prevented downregulation of R_{in}. Asterisks in *C* and *D* marked by post hoc Tukey's test, pairwise comparison followed by 2-way repeated-measures ANOVA, compared with deprived and deprived + BAY or deprived + CP. Asterisks in *E* marked by 2-sample *t*-test. $*P < 0.05$, $**P < 0.01$, $***P < 0.001$; n.s., no significance.

receptor. The I_h density in the control and deprived neurons was measured after treatment with BAY or CP as described in Fig. 2 (Fig. 5). Homeostatic regulation of I_h was restrained by treatment with the mGlu$_1$ receptor inverse agonist, BAY (Fig. 5*A*; control + BAY I_h density = -1.1 ± 0.1 pF, $n = 13$; deprived + BAY I_h density = -1.0 ± 0.2 pF, $n = 13$, at $V_m = -100$ mV; control + BAY vs. deprived + BAY: $P = 0.6$; deprived vs. deprived + BAY: $P < 0.001$, two-way repeated-measured ANOVA). On the other hand, the mGlu$_1$ receptor neutral antagonist did not prevent the homeostatic changes of I_h (Fig. 5*B*; control + CP I_h density = -0.9 ± 0.1 pF at $V_m = -100$ mV, $n = 13$; deprived + CP I_h density = -1.5 ± 0.1 pF, $n = 13$; control + CP vs. deprived + CP: $P < 0.001$; deprived vs. deprived + CP: $P = 0.5$, two-way repeated-measures ANOVA). These findings suggest that the agonist-independent activity of the mGlu$_1$ receptor plays a pivotal role in homeostatic intrinsic plasticity through I_h.

Upstream regulators of I_h have been identified, including PKA (Narayanan et al. 2010), Ca^{2+} calmodulin-dependent protein kinase (CaMKII) (Fan et al. 2005) and auxiliary sub-

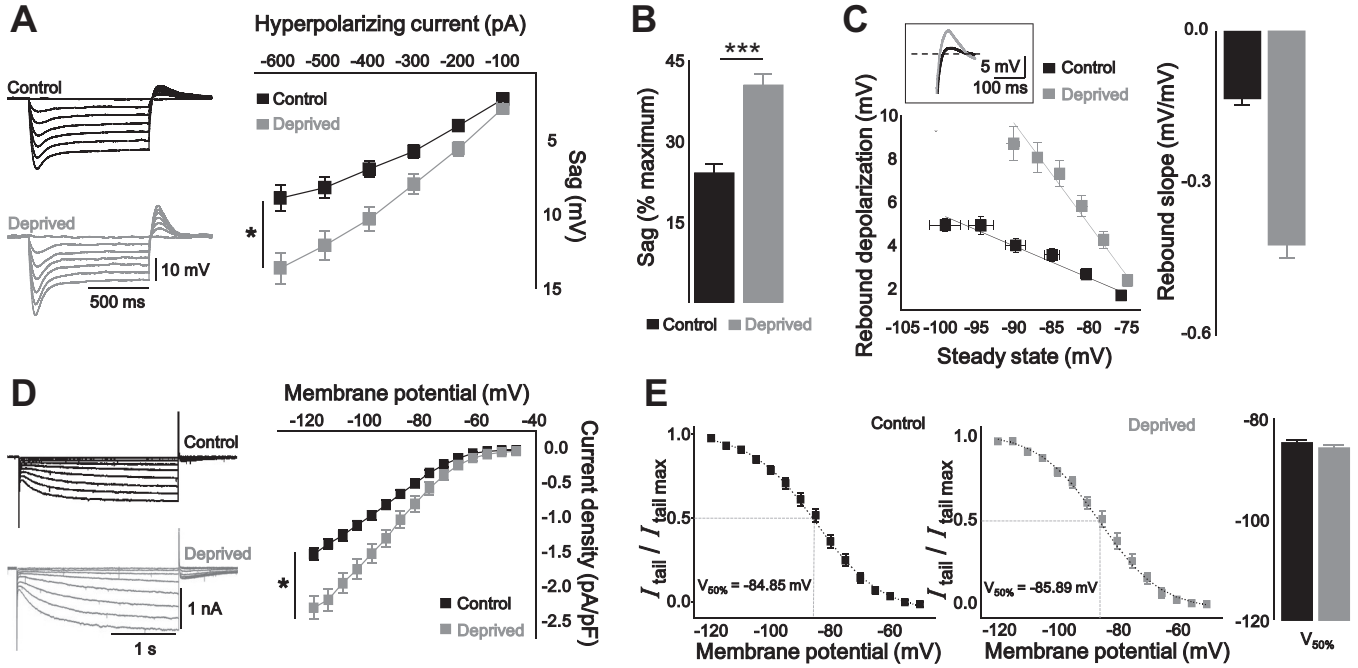

Fig. 3. Activity deprivation resulted in enhanced hyperpolarization-activated current (I_h) activity. *A*: representative traces (*left*) and plots (*right*) showing that voltage sag was significantly increased in deprived neurons (gray) vs. control (black). *B*: bar graph of normalized sag voltage by maximal potential showing the increased voltage sag in deprived neurons. *C*: representative traces (*inset*), plot (*bottom*), and bar graph (*right*) showing relationship between rebound depolarization and steady-state voltage and calculated rebound slope from control and deprived. *D*: representative traces (*left*) and plots (*right*) showing that I_h density was increased in deprived neurons vs. control. *E*: representative plots (*left*) showing activation curve of I_h from control and deprived neurons. Tail current was normalized by maximal tail current amplitude and fitted by Boltzmann function. Bar graph (*right*) showing the half-maximal activation voltage of I_h in control and deprived neurons. Asterisks in *A* and *D* marked by 2-way repeated-measures ANOVA; $*P < 0.05$, $***P < 0.001$.

unit TRIP8B (Santoro et al. 2004). Although the G_q-type of G protein is primarily involved in the excitatory responses of cerebellar PCs, coupling of the mGlu$_1$ receptor to G_S protein activates adenylyl cyclase, and thus, cAMP accumulates resulting in the activation of PKA (Aramori and Nakanishi 1992; Sugiyama et al. 2008; Tateyama and Kubo 2006). Therefore, we asked whether PKA activation is required for the homeostatic control of firing rates in cerebellar PCs. Organotypic slice cultures were chronically treated with a 500 nM PKA inhibitor, (5*R*,6*S*,8*S*)-hexyl 6-hydroxy-5-methyl-13-oxo-6,7,8,13,14,15-hexahydro-5*H*-16-oxa-4b,8a,14-triaza-5,8-methanodibenzo[*b*,*h*]cycloocta[*jkl*]cyclopenta[*e*]-as-indacene-6-carboxylate (KT 5720), in the presence or absence of TTX. The blockade of the PKA activity with KT 5720 (KT) prevented the homeostatic intrinsic plasticity induced by chronic TTX treatment [Fig. 6*A*; firing frequency (Hz): control + KT = 29 ± 3.6, $n = 7$; deprived + KT = 31.9 ± 3.6, $n = 7$ at + 400 pA injection; control + KT vs. deprived + KT, $P = 0.9$; deprived vs. deprived + KT, $P < 0.05$, two-way repeated-measures ANOVA]. In addition, KT also prevented the reduction of R_{in} in TTX-treated neurons (Fig. 6*B*; control + KT = 90.6 ± 2.5 MΩ, $n = 7$; deprived + KT = 83.6 ± 4.8 MΩ, $n = 7$; control + KT vs. deprived + KT, $P = 0.2$, deprived vs. deprived + KT, $P < 0.005$, two-sample *t*-test). This observation indicates that PKA activation mediates homeostatic intrinsic plasticity in cerebellar PCs.

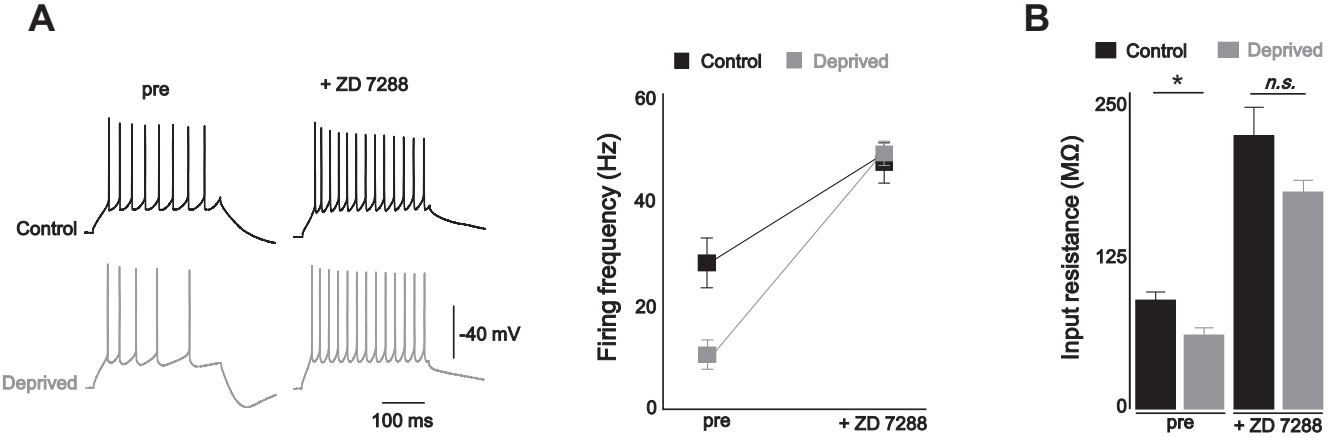

Fig. 4. Blockade of I_h abolished the homeostatic downregulation of firing frequency. *A*: representative traces (*left*) and summarizing plot (*right*) showing that decrease in the intrinsic excitability of the deprived (gray) neurons was restored to control (black) in ZD 7288. *B*: bar graph showing the decrease in R_{in} in deprived neurons was abolished by ZD 7288. Asterisks in *B* marked by 2-sample *t*-test; $*P < 0.05$; n.s., no significance.

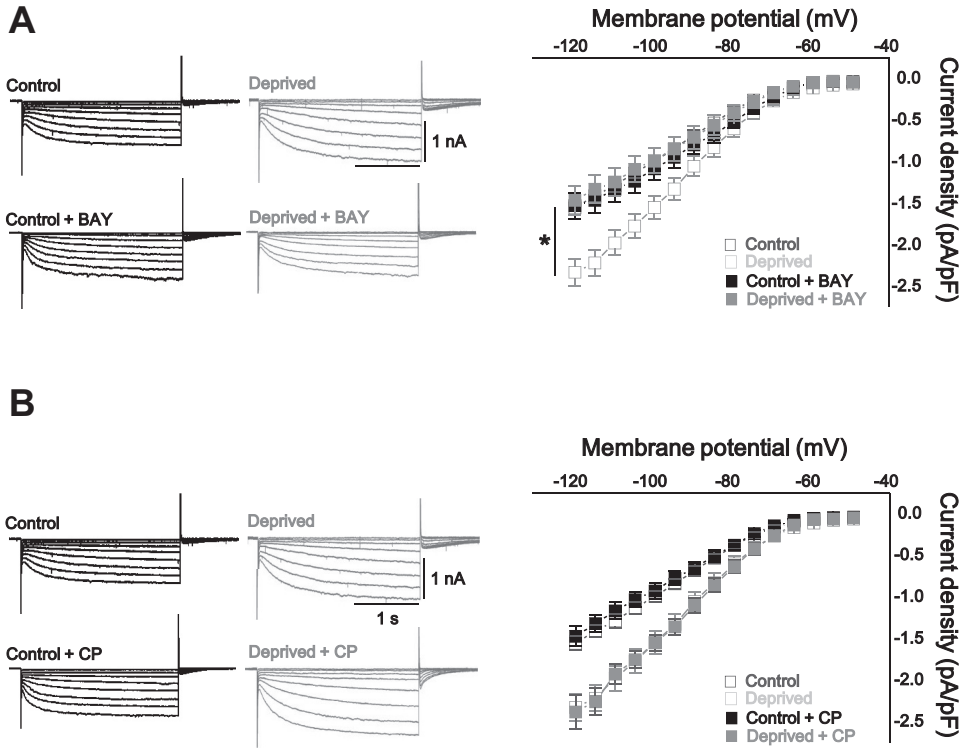

Fig. 5. Homeostatic modulation of I_h required agonist-independent activity of $mGlu_1$ receptor. *A*: representative traces (*left*) and summarizing graph (*right*) showing that inverse agonist of $mGlu_1$ receptor, BAY, prevented homeostatic downregulation of I_h. *B*: representative traces (*left*) and summarizing graph (*right*) showing that there were no effects of antagonizing $mGlu_1$ receptor by CP on homeostatic I_h modulation. Closed black square, BAY only (*A*) or CP only (*B*); closed gray square, deprived + BAY (*A*) or deprived + CP (*B*); open black square, control; open gray square, deprived. Control and deprived values are as described in Fig. 3. Asterisks in *A* marked by 2-way repeated-measures ANOVA, compared with deprived and deprived + BAY; $*P < 0.05$.

DISCUSSION

The present study describes a novel mechanism by which homeostatic regulation of intrinsic excitability in PCs is dependent on the mGlu1 receptor under chronic activity deprivation. Interestingly, homeostatic changes in neuronal excitability were prevented by the $mGlu_1$ receptor inverse agonist but not the neutral antagonist indicating that the homeostatic control of intrinsic excitability might require agonist-independent $mGlu_1$ receptor signaling. Agonist-independent activation of group I mGlu receptors is inhibited by the selective noncompetitive antagonists (also called inverse agonists) Bay and 2-methyl-6-(phenylethynyl)-pyridine (MPEP) (Ango et al. 2001; Hu et al. 2010). Furthermore, we pharmacologically showed that the PKA activity, which is downstream of the mGlu1 receptor (Aramori and Nakanishi 1992; Sugiyama et al. 2008; Tateyama and Kubo 2006) in cerebellar PCs, is involved in homeostatic intrinsic plasticity in cerebellar PCs. This study shows how cerebellar PCs regulate their output signals in a homeostatic manner.

The intrinsic excitability of cerebellar PCs is downregulated by chronic activity deprivation. At first glance, this result is contradictory to conventional homeostatic regulation in which prolonged inactivation of the network activity induces boosting the intrinsic excitability or excitatory synaptic drive (Desai et al. 1999; Galante et al. 2000; Jang et al. 2015). However, in GABAergic neurons, it has been observed that synaptic strength (Chang et al. 2010) and firing rates (Sun 2009) decrease in response to days-long inhibition of network activity. Our results are in agreement with previous studies in that cerebellar PCs are GABAergic neurons. This reduced excitability observed in cerebellar PCs after chronic activity blockade with TTX can induce disinhibition of the silenced cerebellar cortex which could efficiently increase the network excitability against chronic activity deprivation. It is not simple to maintain the stability of the neuronal network activity against activity perturbation because neural activity is rather dynamically modulated (Hengen et al. 2013; Keck et al. 2013). For this reason, 2-day inhibition of network activity by TTX has been widely used to induce homeostatic plasticity, however, neural activity can change day to day. Furthermore, the time course to induce plasticity in vivo is greatly different from in vitro. This is the first observation of homeostatic control in cerebellar PCs. However, in vivo models have not yet been postulated and tested. Starting with this study, an in vivo model of homeostatic plasticity in the cerebellar cortex could be developed. Consequently, it could be possible to explore dynamically regulated neural activity in an activity-dependent manner.

In the present study, we suggest that the agonist-independent activity of the $mGlu_1$ receptor is required for the homeostatic intrinsic plasticity of cerebellar PCs. Even in the absence of an agonist, the $mGlu_1$ receptor can be spontaneously activated, similar to other GPCRs (Ango et al. 2001; Roosterman 2014; Scheer et al. 1996). A previous study has shown that the intracellular protein Homer regulates the agonist-independent constitutive activity of the $mGlu_1$ receptor by interacting with partner proteins, such as the SHANK and MAGUK proteins (Tu et al. 1999). Neuronal excitation during synaptic plasticity or manifestation of convulsive seizures results in expression of the immediate early gene Homer1a (Brakeman et al. 1997; Kato et al. 1997), and the interaction between the $mGlu_1$ receptor and long-form Homer proteins, subsequently, is disrupted leading to the constitutive activity of the receptor (Ango et al. 2001). In our experimental conditions in which the network activity is totally suppressed by TTX, there is a minute possibility that Homer 1a is involved in the activity deprivation-driven reduction of excitability because neuronal depolarization commonly induces Homer1a (Minami et al. 2003) but

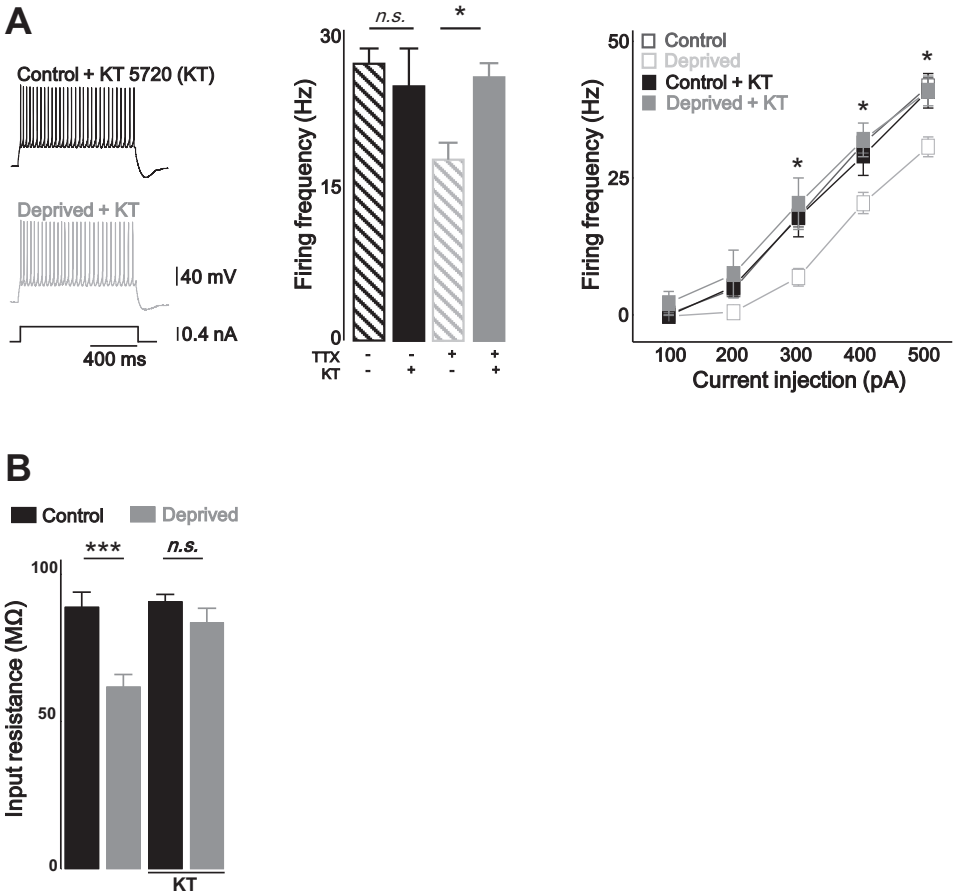

Fig. 6. Homeostatic intrinsic plasticity was dependent on PKA pathway. *A*: representative traces (*left*) and bar graph (*middle*; at +400 pA injection) and plots (*right*) showing that treatment of PKA inhibitor KT 5720 (KT) prevented homeostatic intrinsic plasticity in cerebellar PCs. *B*: bar graph showing the reduced R_{in} was recovered by KT (500 nM). Closed black square, KT only; closed gray square, deprived + KT; open black square, control; open gray square, deprived. Control and deprived values are as described in Fig. 1. Asterisks in *A* marked by post hoc Tukey's test, pairwise comparison followed by 2-way repeated-measures ANOVA, compared with deprived and deprived + KT. Asterisks in *B* marked by 2-sample *t*-test; $*P < 0.05$, $***P < 0.001$; n.s., no significance.

is more rather due to the downregulation of the long-form Homers, which induces the agonist-independent activation of $mGlu_1$ receptors in cerebellar PCs. Indeed, knock-down of Homer3 facilitates the $mGlu_1$ receptor activity by shifting equilibrium between its inactive and active conformation (Ango et al. 2001). The complex receptor-intracellular protein interactions in response to chronic changes in network activity due to neural plasticity and/or pathological conditions need to be further investigated.

The level of GPCR activity, a functional readout of the group I mGlu receptor activity, has been determined by the balance between the inactive (R) and active (R*) form of the receptor (Chidiac et al. 1994). Conformational changes of the receptor from the R to R* are regarded as one of the underlying mechanisms of constitutive activity (Scheer et al. 1996). Alternatively, an increased density of GPCRs enhances the agonist-independent activity of the receptor through an increase in the absolute amount of R* (Smit et al. 1996). We observed that activity-deprivation elevates $mGlu_1$ receptor α, and this may reflect strengthened GPCR signaling through an increased amount of the R* form of the receptor. In addition, when the PKA pathway, downstream of the mGlu1 receptor (Aramori and Nakanishi 1992; Sugiyama et al. 2008; Tateyama and Kubo 2006), is inhibited under activity-deprived conditions, homeostatic intrinsic plasticity is prevented, suggesting that activity deprivation activates PKA. Given that the $mGlu_1$ receptor activates adenylyl cyclase by the coupling of the receptor to the G_S protein and cAMP subsequently accumulates (Tateyama and Kubo 2006), we can conclude that the chronic blockade of network activity activates $mGlu_1$ receptor signaling resulting in the downregulation of firing rates through the PKA pathway. When $mGlu_1$ receptor is activated, various cell responses are induced through coupling to several types of G proteins. Coupling of $mGlu_1$ receptor to G_{q11} can lead to the accumulation of inositol 1,4,5-trisphosphate ($InsP_3$) resulting in the activation of the protein kinase C (PKC) pathway (Francesconi and Duvoisin 2000; Tateyama and Kubo 2006). A previous study reported that PKC activation inhibits I_h (Brager and Johnston 2007; Reetz and Strauss 2013). This leads to an increase in intrinsic excitability which contradicts our observation. Although G_S and G_{q11} coupling is simultaneously and independently triggered by $mGlu_1$ receptor activation, PKA is a more plausible upstream regulator of the elevated I_h. For this reason, we exclude the PKC pathway in homeostatic intrinsic plasticity in cerebellar PCs.

Various ion channels determine the active and passive electrical properties of neuronal membranes, including membrane potential and AP threshold, and contribute to the synaptic integration and firing fidelity. Synaptic stimulus and/or somatic depolarization modifies neuronal excitability by changing the composition and conductance of ion channels (Belmeguenai et al. 2010; Hyun et al. 2013). From a homeostatic viewpoint, ion channels are dynamically regulated (Desai et al. 1999) to acquire network stability, and accordingly, AP firing rates are tuned within suitable ranges. Given the decreased R_{in} in deprived neurons, we focused on I_h among ion channels that contribute to neuronal excitability. However, the activity of many other ion channels need to be measured. A previous

study showed that visual deprivation changes $I_{threshold}$ not $V_{threshold}$, and R_{in} which is in agreement with our results (Fig. 1, Table 1) (Nataraj et al. 2010). Hence TEA-sensitive delayed-rectifier type K^+ channel (K_V 2.1) are a possible candidate for determining the excitability. Although Ca^{2+}-activated K^+ channels can be involved in homeostatic intrinsic plasticity, these are excluded because they have less of an effect on R_{in} and $I_{threshold}$ (Belmeguenai et al. 2010).

HCN channels are widely expressed in several brain regions (Notomi and Shigemoto 2004), and they contribute to the regulation of neural activity. Because I_h generates a tonic inward current at resting state, it is known as a pacemaker to initiate neuronal oscillation and rhythmic burst activity (Jahnsen and Llinas 1984; Llinas and Jahnsen 1982; Mccormick and Pape 1990). A previous study showed that the pharmacological blockade of I_h modifies membrane bistability, thereby inducing the spontaneous quiescence period (Williams et al. 2002). This indicates that I_h maintains the membrane potential, which enables tonic AP activity even when the activity of PCs is disrupted by hyperpolarizing inputs. Given that I_h stabilizes the cellular membrane potential within an appropriate range by its unusual gating properties (Nolan et al. 2007), activity-dependent regulation of I_h will be essential for homeostatic plasticity in an activity-disturbance condition. Homeostatically elevated I_h reduces R_{in} leading to a dampened membrane deflection to given current stimulation, and this will act as a cellular stabilizer to preserve the membrane potential. Furthermore, a potentiated rebound potential keeps the membrane potential close to the AP threshold and consequently leads to 'history-independent integration' (Nolan et al. 2003). Therefore, we suggest that the activity of cerebellar PCs is fine-tuned by the consequences of I_h modulation when the network activity is deprived.

Homeostatic plasticity has been regarded as a key mechanism of disease initiation (Friedman et al. 2014). Chronic activity-deprivation reduces the firing rates of cerebellar PCs, and it could be related to cerebellar disorders including Friedreich ataxia and spinocerebellar ataxias (SCAs) because lowered excitability is linked to the cellular phenomenon of disease (Hourez et al. 2011). Given that the constitutive activity of GPCRs is correlated to various human diseases, this work provides insight into possible therapeutic targets though modulation of GPCR-mediated homeostatic intrinsic plasticity. In addition, we also provide insight into the cellular basis of homeostatic control of firing rates of cerebellar PCs, and this finding broadens the understanding of homeostatic intrinsic plasticity of the cerebellar cortex.

ACKNOWLEDGMENTS

We thank Misun Mun, Geehoon Chung, and Michael Chang for proofreading the manuscript and providing scientific advice.

GRANTS

This study was supported by National Research Foundation of Korea (NRF) Grant funded by the Korean government (MSIP) 2012R1A5A2A44671346; Korean Health Technology R&D Project, Ministry of Health & Welfare (A120476); and the Basic Science Research Program through the NRF funded by Ministry of Education Grant 2013R1A1A2013184.

DISCLOSURES

No conflicts of interest, financial or otherwise, are declared by the author(s).

AUTHOR CONTRIBUTIONS

Author contributions: H.G.S., S.-S.J., J.M.P., and S.J.K. conception and design of research; H.G.S. and D.C.J. performed experiments; H.G.S. and D.C.J. analyzed data; H.G.S., D.C.J., J.M.P., and S.J.K. interpreted results of experiments; H.G.S., J.M.P., and S.J.K. prepared figures; H.G.S., D.C.J., J.M.P., and S.J.K. drafted manuscript; H.G.S., S.-S.J., D.C.J., Y.J., W.C., J.M.P., and S.J.K. edited and revised manuscript; H.G.S., S.-S.J., D.C.J., Y.J., W.C., J.M.P., and S.J.K. approved final version of manuscript.

REFERENCES

Ango F, Prezeau L, Muller T, Tu JC, Xiao B, Worley PF, Pin JP, Bockaert J, Fagni L. Agonist-independent activation of metabotropic glutamate receptors by the intracellular protein Homer. *Nature* 411: 962–965, 2001.

Aramori I, Nakanishi S. Signal transduction and pharmacological characteristics of a metabotropic glutamate receptor, mGluR1, in transfected CHO cells. *Neuron* 8: 757–765, 1992.

Belmeguenai A, Hosy E, Bengtsson F, Pedroarena CM, Piochon C, Teuling E, He Q, Ohtsuki G, De Jeu MT, Elgersma Y, De Zeeuw CI, Jorntell H, Hansel C. Intrinsic plasticity complements long-term potentiation in parallel fiber input gain control in cerebellar Purkinje cells. *J Neurosci* 30: 13630–13643, 2010.

Beraneck M, Idoux E. Reconsidering the role of neuronal intrinsic properties and neuromodulation in vestibular homeostasis. *Front Neurol* 3: 25, 2012.

Brager DH, Johnston D. Plasticity of intrinsic excitability during long-term depression is mediated through mGluR-dependent changes in I(h) in hippocampal CA1 pyramidal neurons. *J Neurosci* 27: 13926–13937, 2007.

Brakeman PR, Lanahan AA, O'Brien R, Roche K, Barnes CA, Huganir RL, Worley PF. Homer: a protein that selectively binds metabotropic glutamate receptors. *Nature* 386: 284–288, 1997.

Campanac E, Daoudal G, Ankri N, Debanne D. Downregulation of dendritic I(h) in CA1 pyramidal neurons after LTP. *J Neurosci* 28: 8635–8643, 2008.

Chang MC, Park JM, Pelkey KA, Grabenstatter HL, Xu D, Linden DJ, Sutula TP, McBain CJ, Worley PF. Narp regulates homeostatic scaling of excitatory synapses on parvalbumin-expressing interneurons. *Nat Neurosci* 13: 1090–1097, 2010.

Chidiac P, Hebert TE, Valiquette M, Dennis M, Bouvier M. Inverse agonist activity of beta-adrenergic antagonists. *Mol Pharmacol* 45: 490–499, 1994.

Desai NS, Rutherford LC, Turrigiano GG. Plasticity in the intrinsic excitability of cortical pyramidal neurons. *Nat Neurosci* 2: 515–520, 1999.

Ehlers MD. Activity level controls postsynaptic composition and signaling via the ubiquitin-proteasome system. *Nat Neurosci* 6: 231–242, 2003.

Fan Y, Fricker D, Brager DH, Chen X, Lu HC, Chitwood RA, Johnston D. Activity-dependent decrease of excitability in rat hippocampal neurons through increases in I(h). *Nat Neurosci* 8: 1542–1551, 2005.

Francesconi A, Duvoisin RM. Opposing effects of protein kinase C and protein kinase A on metabotropic glutamate receptor signaling: selective desensitization of the inositol trisphosphate/Ca2+ pathway by phosphorylation of the receptor-G protein-coupling domain. *Proc Natl Acad Sci USA* 97: 6185–6190, 2000.

Friedman AK, Walsh JJ, Juarez B, Ku SM, Chaudhury D, Wang J, Li X, Dietz DM, Pan N, Vialou VF, Neve RL, Yue Z, Han MH. Enhancing depression mechanisms in midbrain dopamine neurons achieves homeostatic resilience. *Science* 344: 313–319, 2014.

Galante M, Nistri A, Ballerini L. Opposite changes in synaptic activity of organotypic rat spinal cord cultures after chronic block of AMPA/kainate or glycine and GABAA receptors. *J Physiol* 523: 639–651, 2000.

Hengen KB, Lambo ME, Van Hooser SD, Katz DB, Turrigiano GG. Firing rate homeostasis in visual cortex of freely behaving rodents. *Neuron* 80: 335–342, 2013.

Hourez R, Servais L, Orduz D, Gall D, Millard I, de Kerchove d'Exaerde A, Cheron G, Orr HT, Pandolfo M, Schiffmann SN. Aminopyridines correct early dysfunction and delay neurodegeneration in a mouse model of spinocerebellar ataxia type 1. *J Neurosci*: 11795–11807, 2011.

Hu JH, Park JM, Park S, Xiao B, Dehoff MH, Kim S, Hayashi T, Schwarz MK, Huganir RL, Seeburg PH, Linden DJ, Worley PF. Homeostatic scaling requires group I mGluR activation mediated by Homer1a. *Neuron* 68: 1128–1142, 2010.

Hyun JH, Eom K, Lee KH, Ho WK, Lee SH. Activity-dependent down-regulation of D-type K^+ channel subunit Kv1.2 in rat hippocampal CA3 pyramidal neurons. *J Physiol* 591: 5525–5540, 2013.

Jahnsen H, Llinas R. Ionic basis for the electroresponsiveness and oscillatory properties of guinea-pig thalamic neurons invitro. *J Physiol* 349: 227–247, 1984.

Jang SS, Royston SE, Xu J, Cavaretta JP, Vest MO, Lee KY, Lee S, Jeong HG, Lombroso PJ, Chung HJ. Regulation of STEP61 and tyrosine-phosphorylation of NMDA and AMPA receptors during homeostatic synaptic plasticity. *Mol Brain* 8: 55, 2015.

Kammermeier PJ, Xiao B, Tu JC, Worley PF, Ikeda SR. Homer proteins regulate coupling of group I metabotropic glutamate receptors to N-type calcium and M-type potassium channels. *J Neurosci* 20: 7238–7245, 2000.

Kato A, Ozawa F, Saitoh Y, Hirai K, Inokuchi K. vesl, a gene encoding VASP/Ena family related protein, is upregulated during seizure, long-term potentiation and synaptogenesis. *FEBS Lett* 412: 183–189, 1997.

Keck T, Keller GB, Jacobsen RI, Eysel UT, Bonhoeffer T, Hubener M. Synaptic scaling and homeostatic plasticity in the mouse visual cortex in vivo. *Neuron* 80: 327–334, 2013.

Lambo ME, Turrigiano GG. Synaptic and intrinsic homeostatic mechanisms cooperate to increase L2/3 pyramidal neuron excitability during a late phase of critical period plasticity. *J Neurosci* 33: 8810–8819, 2013.

Lee KY, Royston SE, Vest MO, Ley DJ, Lee S, Bolton EC, Chung HJ. N-methyl-D-aspartate receptors mediate activity-dependent down-regulation of potassium channel genes during the expression of homeostatic intrinsic plasticity. *Mol Brain* 8: 4, 2015.

Litschig S, Gasparini F, Rueegg D, Stoehr N, Flor PJ, Vranesic I, Prezeau L, Pin JP, Thomsen C, Kuhn R. CPCCOEt, a noncompetitive metabotropic glutamate receptor 1 antagonist, inhibits receptor signaling without affecting glutamate binding. *Mol Pharmacol* 55: 453–461, 1999.

Llinas R, Jahnsen H. Electrophysiology of mammalian thalamic neurons in vitro. *Nature* 297: 406–408, 1982.

Mccormick DA, Pape HC. Noradrenergic and serotonergic modulation of a hyperpolarization-activated cation current in thalamic relay neurons. *J Physiol* 431: 319–342, 1990.

Minami I, Kengaku M, Smitt PS, Shigemoto R, Hirano T. Long-term potentiation of mGluR1 activity by depolarization-induced Homer1a in mouse cerebellar Purkinje neurons. *Eur J Neurosci* 17: 1023–1032, 2003.

Nakashima A, Takeuchi H, Imai T, Saito H, Kiyonari H, Abe T, Chen M, Weinstein LS, Yu CR, Storm DR, Nishizumi H, Sakano H. Agonist-independent GPCR activity regulates anterior-posterior targeting of olfactory sensory neurons. *Cell* 154: 1314–1325, 2013.

Narayanan R, Dougherty KJ, Johnston D. Calcium store depletion induces persistent perisomatic increases in the functional density of h channels in hippocampal pyramidal neurons. *Neuron* 68: 921–935, 2010.

Nataraj K, Le Roux N, Nahmani M, Lefort S, Turrigiano G. Visual deprivation suppresses L5 pyramidal neuron excitability by preventing the induction of intrinsic plasticity. *Neuron* 68: 750–762, 2010.

Naude J, Cessac B, Berry H, Delord B. Effects of cellular homeostatic intrinsic plasticity on dynamical and computational properties of biological recurrent neural networks. *J Neurosci* 33: 15032–15043, 2013.

Nolan MF, Dudman JT, Dodson PD, Santoro B. HCN1 channels control resting and active integrative properties of stellate cells from layer II of the entorhinal cortex. *J Neurosci* 27: 12440–12451, 2007.

Nolan MF, Malleret G, Lee KH, Gibbs E, Dudman JT, Santoro B, Yin DQ, Thompson RF, Siegelbaum SA, Kandel ER, Morozov A. The hyperpolarization-activated HCN1 channel is important for motor learning and neuronal integration by cerebellar Purkinje cells. *Cell* 115: 551–564, 2003.

Notomi T, Shigemoto R. Immunohistochemical localization of Ih channel subunits, HCN1-4, in the rat brain. *J Comp Neurol* 471: 241–276, 2004.

O'Leary T, Williams AH, Franci A, Marder E. Cell types, network homeostasis, and pathological compensation from a biologically plausible ion channel expression model. *Neuron* 82: 809–821, 2014.

Reetz O, Strauss U. Protein kinase C activation inhibits rat and human hyperpolarization activated cyclic nucleotide gated channel (HCN)1-mediated current in mammalian cells. *Cell Physiol Biochem* 31: 532–541, 2013.

Roosterman D. Agonist-dependent and -independent dopamine-1-like receptor signalling differentially regulates downstream effectors. *FEBS J* 281: 4792–4804, 2014.

Rosenkranz JA, Johnston D. Dopaminergic regulation of neuronal excitability through modulation of Ih in layer V entorhinal cortex. *J Neurosci* 26: 3229–3244, 2006.

Santoro B, Wainger BJ, Siegelbaum SA. Regulation of HCN channel surface expression by a novel C-terminal protein-protein interaction. *J Neurosci* 24: 10750–10762, 2004.

Scheer A, Fanelli F, Costa T, De Benedetti PG, Cotecchia S. Constitutively active mutants of the alpha 1B-adrenergic receptor: role of highly conserved polar amino acids in receptor activation. *EMBO J* 15: 3566–3578, 1996.

Shepherd JD, Rumbaugh G, Wu J, Chowdhury S, Plath N, Kuhl D, Huganir RL, Worley PF. Arc/Arg3.1 mediates homeostatic synaptic scaling of AMPA receptors. *Neuron* 52: 475–484, 2006.

Smit MJ, Leurs R, Alewijnse AE, Blauw J, Van Nieuw Amerongen GP, Van De Vrede Y, Roovers E, Timmerman H. Inverse agonism of histamine H2 antagonist accounts for upregulation of spontaneously active histamine H2 receptors. *Proc Natl Acad Sci USA* 93: 6802–6807, 1996.

Stemmler M, Koch C. How voltage-dependent conductances can adapt to maximize the information encoded by neuronal firing rate. *Nat Neurosci* 2: 521–527, 1999.

Sugiyama Y, Kawaguchi SY, Hirano T. mGluR1-mediated facilitation of long-term potentiation at inhibitory synapses on a cerebellar Purkinje neuron. *Eur J Neurosci* 27: 884–896, 2008.

Sun QQ. Experience-dependent intrinsic plasticity in interneurons of barrel cortex layer IV. *J Neurophysiol* 102: 2955–2973, 2009.

Sutton MA, Taylor AM, Ito HT, Pham A, Schuman EM. Postsynaptic decoding of neural activity: eEF2 as a biochemical sensor coupling miniature synaptic transmission to local protein synthesis. *Neuron* 55: 648–661, 2007.

Tateyama M, Kubo Y. Dual signaling is differentially activated by different active states of the metabotropic glutamate receptor 1alpha. *Proc Natl Acad Sci USA* 103: 1124–1128, 2006.

Tu JC, Xiao B, Naisbitt S, Yuan JP, Petralia RS, Brakeman P, Doan A, Aakalu VK, Lanahan AA, Sheng M, Worley PF. Coupling of mGluR/Homer and PSD-95 complexes by the Shank family of postsynaptic density proteins. *Neuron* 23: 583–592, 1999.

Williams SR, Christensen SR, Stuart GJ, Hausser M. Membrane potential bistability is controlled by the hyperpolarization-activated current I(H) in rat cerebellar Purkinje neurons in vitro. *J Physiol* 539: 469–483, 2002.